KfK 2893
AECL-6420
Oktober 1980

The Development of a Burst Criterion for Zircaloy Fuel Cladding under LOCA Conditions

H. J. Neitzel, H. E. Rosinger
Institut für Reaktorbauelemente

Kernforschungszentrum Karlsruhe

KERNFORSCHUNGSZENTRUM KARLSRUHE
Institut für Reaktorbauelemente

KfK 2893
(AECL - 6420)

THE DEVELOPMENT OF A BURST CRITERION FOR ZIRCALOY FUEL CLADDING UNDER LOCA CONDITIONS

H. J. Neitzel, H. E. Rosinger[x)]

x) Visiting scientist at KfK from January to August 1979
Atomic Energy of Canada Limited, Whiteshell Nuclear
Research Establishment, Pinawa, Manitoba, ROE 1LO

Kernforschungszentrum Karlsruhe GmbH, Karlsruhe

Kernforschungszentrum Karlsruhe GmbH
ISSN 0303-4003

Abstract

A burst criterion model, which assumes that deformation is controlled by steady-state creep, has been developed for a thin-walled cladding, in this case Zircaloy-4, subjected to a differential pressure and high temperature. The creep equation is integrated to obtain a burst time at the singularity of the strain. Once that burst time is known, the burst temperature and burst pressure can be calculated from the known temperature and pressure histories. A further relationship between burst stress and burst temperature is used to calculate the burst strain.

Comparison with measured burst data shows good agreement between theory and experiment. It was found that, if the heating rate is constant, the burst temperature increases with decreasing stress, and that, if the stress level is constant, the burst temperature increases with increasing heating rate. It was also found that anisotropy alters the burst temperature and burst strain, and that test conditions in the α-Zr temperature range have no influence on the burst data.

Zusammenfassung

Entwicklung eines Berstkriteriums für Zirkaloy-Hüllrohre unter LOCA-Bedingungen

Zur Berechnung der Berstdaten für Zirkaloy-Hüllrohre unter LOCA-Bedingungen wurde ein Berstkriterium entwickelt, welches davon ausgeht, daß der zeitliche Dehnungsverlauf zum Berstzeitpunkt ins Unendliche strebt. Dabei wurde angenommen, daß die Deformation durch sekundäres Kriechen bestimmt wird. Durch Integration der Kriechbeziehung bis zur Singularität in der Dehnung erhält man die Berstzeit. Bei bekannter Berstzeit kann über die gegebenen zeitlichen Funktionen für Temperatur und Druck Bersttemperatur und Berstdruck berechnet werden. Eine empirische Beziehung zwischen Berstspannung und Temperatur gestattet es sodann, Berstspannung und Berstdehnung zu berechnen.

Ein Vergleich mit gemessenen Berstdaten zeigt eine gute Übereinstimmung zwischen Theorie und Messung.

CONTENTS

LIST OF SYMBOLS

Symbol	Definition	Dimension
t	time	s
T	absolute temperature	K
P	pressure	MPa
$\dot{\varepsilon}$	steady-state strain rate or creep rate	s^{-1}
ε	strain	1
A	structure parameter	$(MPa)^{-1} \cdot s^{-1}$
Q	activation energy	$J \cdot mol^{-1}$
k	absolute gas constant	$J \cdot mol^{-1} \cdot K^{-1}$
σ	stress	MPa
n	stress exponent of the creep rate	1
R	mean tube radius	mm
s	tube wall thickness	mm
a	1. burst stress parameter	MPa
b	2. burst stress parameter	K^{-1}
F,G,H	anisotropy coefficients for the normal stress components in the Hill equation	1
σ_f	effective stress	MPa

Subscripts

o	initial condition
B	burst
$*$	singularity
θ	tangential direction
r	radial direction
Z	axial direction

1. INTRODUCTION

Subjecting a thin-walled tube to high temperature and a positive internal pressure will cause the tube to strain. Under the proper conditions the differential pressure may cause severe deformation and, finally, bursting (rupture, failure) of the tube. In this work we have developed a simple model to calculate the burst temperature and burst strain of a thin-walled tube subjected to high temperature and a differential pressure. In particular, we have employed the model to calculate the burst temperatures and burst strains of Zircaloy-4 fuel cladding subjected to temperatures and pressures that might be expected in a hypothetical Loss-of-Coolant Accident (LOCA) in a water-cooled reactor.

In the burst criterion model the steady-state creep equation is integrated to obtain the strain as a function of the time. Eventually, a singularity in the strain is reached at which time, t_B^*, the strain tends to infinity. Since the strain cannot in reality go to infinity, this time t_B^* is not the exact burst time. However, because of the rapid increase in strain for very small increases in time near the burst point, it can be assumed that the time t_B^* at the singularity corresponds approximately to the burst time t_B. The burst temperature T_B and burst pressure P_B can be calculated from the burst time t_B^*, if the material properties (A, n, Q) of the steady-state creep equations as well as the pressure and temperature histories as functions of time are known. The pressure and temperature histories are obtained by experiment or calculated using computer codes such as SSYT[1], FRAP-T[2] or FAXMOD[3,4].

In order to determine the burst strain, a further empirical relationship is employed. Relationships have been established between burst temperature and burst stress or burst strain. Because experimental scatter of burst stress is considerably less than that of burst

strain, the relationship between burst stress and burst temperature, developed by Brzoska et al.[5], is used to calculate the burst strain.

The burst criterion is developed for symmetrical tube deformation. It can, however, in principle, be used for asymmetrical deformation as might be found when azimuthal temperature variations exist. In this case, the burst criterion must be applied locally to calculate the singularity.

2. THEORETICAL RELATIONSHIPS

2.1 BASIC EQUATIONS

The present model assumes that the burst data for internally pressurized Zircaloy cladding can be calculated from the steady-state (secondary) creep equation of the material. The steady-state creep rate of a material at constant temperature and constant stress can usually be represented by a power law - Arrhenius equation (the so-called Norton equation) of the form:

$$\dot{\varepsilon} = \frac{d\varepsilon}{dt} = A \cdot \exp\left[\frac{-Q}{kT}\right] \cdot \sigma^n \qquad (1)$$

where $\dot{\varepsilon}$ is the steady-state strain rate, or creep rate, s^{-1}

ε is the strain

t is the time, s

A is a structure parameter, $(MPa)^{-n} \cdot s^{-1}$

Q is the activation energy, $J \cdot mol^{-1}$

k is the absolute gas constant, $k = 8.315\ J \cdot mol^{-1} \cdot K^{-1}$

T is the absolute temperature, K

σ is the applied stress, MPa

n is the stress exponent.

For symmetrical deformation, the tangential stress (also termed hoop stress) for a thin-walled tube under a differential pressure P is given by:

$$\sigma = P \cdot R/s \tag{2}$$

where R is the instantaneous mean tube radius

s is the instantaneous tube wall thickness.

If the instantaneous tangential strain is defined by:

$$R = R_o (1 + \varepsilon) \tag{3}$$

where R_o is the original mean tube radius, it can be shown that the tangential stress σ at any time changes with the tangential strain ε according to the equation:

$$\sigma = \frac{P}{P_o} \cdot \sigma_o \cdot (1 + \varepsilon)^2 \tag{4}$$

where P is the actual pressure, MPa

P_o is the initial pressure, MPa

σ_o is the initial stress, MPa

ε is the tangential or diametral strain.

It is assumed that there is no axial shortening and that a constant cross-sectional area is maintained.

Substituting equation (4) into (1) and rearranging terms, one obtains the differential equation for the diametral strain:

$$\frac{d\varepsilon}{(1 + \varepsilon)^{2n}} = A \left(\frac{P}{P_o}\right)^n \cdot \exp\left(\frac{-Q}{kT}\right) \cdot \sigma_o^{\,n} \cdot dt \tag{5}$$

It is the solution, and interpretation, of this equation that forms the basis for this report.

For any specified history of pressure P(t) and temperature T(t) and known values of A, n and Q, it is possible, by integrating equation (5), to calculate the tangential strain as a function of time. This tangential strain in general has a singularity at which point the strain increases to infinity, i.e., $\varepsilon \to \infty$, and a time t_B^* is obtained - see Figure 1. The actual strain, however, cannot tend to infinity and hence the actual burst time t_B is somewhat lower than t_B^*. The absolute time difference between t_B and t_B^* is small and can be ignored for most practical cases. Once the burst time is known, the burst temperature T_B and the burst pressure P_B can be calculated from the temperature- and pressure-time histories.

According to equation (4), the stress also approaches infinity as the strain approaches infinity. This is again not possible. In agreement with Brzoska et al.[5], we assume that the boundary for the burst stress σ_B is given by:

$$\sigma_B = a \cdot \exp(-bT_B) \qquad (6)$$

where a and b are experimentally determined constants. This equation states that the burst stress is mainly temperature dependent. The experimentally determined values a and b[5] may be influenced by other parameters such as the heating rate or test atmosphere.

The burst temperature T_B and the burst pressure P_B can be calculated by integrating the differential equation (5) to the singularity. The burst stress σ_B can be calculated from equation (6) and the burst strain ε_B can be calculated from equation (4) knowing burst pressure P_B. Then the burst strain can be calculated from equations (4) and (6) as:

$$\varepsilon_B = \left[\frac{P_o}{P_B} \cdot \frac{a}{\sigma_o} \cdot \exp(-bT_B)\right]^{\frac{1}{2}} - 1 \qquad (7)$$

It should be noted that the burst strain ε_B is dependent on the pressure P(t) and temperature T(t) histories because the burst pressure P_B and burst temperature T_B are obtained by the integration of equation (5) which contains these histories.

2.2 MULTIAXIAL STRESS STATE AND ANISOTROPY

According to Hunt[6], Lukas[7] and Ross-Ross et al.[8], the creep rate of anisotropic materials can be deduced from the Hill[9] theory for anisotropy as:

$$\begin{aligned}
\dot{\varepsilon}_r &= \dot{\varepsilon}_f \cdot [H(\sigma_r - \sigma_\theta) - G(\sigma_z - \sigma_r)]/\sigma_f \\
\dot{\varepsilon}_\theta &= \dot{\varepsilon}_f \cdot [F(\sigma_\theta - \sigma_z) - H(\sigma_r - \sigma_\theta)]/\sigma_f \qquad (8) \\
\dot{\varepsilon}_z &= \dot{\varepsilon}_f \cdot [G(\sigma_z - \sigma_r) - F(\sigma_\theta - \sigma_z)]/\sigma_f
\end{aligned}$$

where the subscripts r, θ and z refer to the radial, tangential and axial directions, respectively. σ_f and $\dot{\varepsilon}_f$ are the effective stress and effective creep rate and F, G and H are the anisotropic factors as defined by Hill[9].

If the axes of anisotropy coincide with the axes of principal stress, then the effective stress is given by:

$$\sigma_f = [F(\sigma_\theta - \sigma_z)^2 + G(\sigma_z - \sigma_r)^2 + H(\sigma_r - \sigma_\theta)^2]^{\frac{1}{2}} \qquad (9)$$

The effective creep rate can be eliminated in equation (8) by assuming the following power-law relationship between the effective creep rate and effective stress:

$$\dot{\varepsilon}_f = A_f \cdot \exp\left(\frac{-Q}{kT}\right) \cdot \sigma_f^{\,n} \tag{10}$$

In this equation it is assumed that the same deformation mechanism is responsible for all the deformations and that it is direction independent.

From equation (8) the following relationships may be derived:

1. For a creep specimen uniaxially stressed by σ_z, $\sigma_\theta = \sigma_r = 0$, if the uniaxial stress-creep rate relationship is given by:

$$\dot{\varepsilon}_z = A_z \cdot \exp\left(\frac{-Q}{kT}\right) \cdot \sigma_z^{\,n} \tag{11}$$

then from equations (8) to (11) it can be shown that:

$$A_f = \frac{A_z}{(F + G)^{(n+1)/2}} \tag{12}$$

2. For a thin-walled (closed-end) tube under an internal pressure only, $\sigma_z = \sigma_\theta/2$, $\sigma_r = 0$, and with:

$$\dot{\varepsilon}_\theta = A_\theta \cdot \exp\left(\frac{-Q}{kT}\right) \cdot \sigma_\theta^{\,n} \tag{13}$$

it can be shown that:

$$A_\theta = \left(\frac{F + G}{4} + H\right)^{(n-1)/2} \cdot (H + 0.5F) \cdot A_f \tag{14}$$

Since the values of A_f, n and Q are determined from uniaxial creep tests[10] and the data are applied to tube tests, care must be taken to employ the proper corrections, i.e., a combination of equations (12) and (14):

$$A_\theta = (F + G)^{-(n+1)/2} \cdot \left(\frac{F + G}{4} + H\right)^{(n-1)/2} \cdot (H + 0.5F) \cdot A_z \qquad (15)$$

2.3 BURST CRITERION

Although an analytical solution for equation (5) is possible for constant material properties (A, n, Q) and simple histories of pressure and temperature, the numerical solution would normally be employed to avoid any restrictions on the use of the equation.

The integration of equation (5) is carried out for a small time step Δt. During the time step the material properties, pressure P(t) and temperature T(t) are considered as being constant and, specifically, they assume their constant value at the time $(t + \Delta t/2)$.

If one further assumes that the property parameters are functions of temperature, which is a function of time, then by implication the property parameters are indirectly time dependent. The integration is carried out between the times t_1 and $t_2 = t_1 + \Delta t$. The corresponding strain values are ε_1 and $\varepsilon_2 = \varepsilon_1 + \Delta\varepsilon$. From equation (5) one obtains:

$$-\frac{1}{2n_{12} - 1} \cdot \frac{1}{(1 + \varepsilon^*)^{(2n_{12}-1)}} \Bigg|_{\varepsilon_1}^{\varepsilon_1 + \Delta\varepsilon} = \Delta I \qquad (16)$$

where:

$$\Delta I = A_{12} \left(\frac{P_{12}}{P_o}\right)^{n_{12}} \cdot \sigma_o{}^{n_{12}} \cdot \exp\left(\frac{-Q_{12}}{kT_{12}}\right)\Delta t \qquad (17)$$

and the subscript 12 refers to the value at $t_1 + \Delta t/2$.

From equation (16) one obtains:

$$\frac{1}{(1+\varepsilon_2)^{(2n_{12}-1)}} - \frac{1}{(1+\varepsilon_1)^{(2n_{12}-1)}} = -(2n_{12}-1)\cdot\Delta I$$

or

$$\varepsilon_2 = \left\{ \frac{1}{\frac{1}{(1+\varepsilon_1)^{(2n_{12}-1)}} - (2n_{12}-1)\Delta I} \right\}^{\frac{1}{2n_{12}-1}} - 1 \qquad (18)$$

As a result of equation (16), the new strain ε_2 has a singularity when the denominator in the equation is zero. That is, burst occurs when the condition:

$$(2n_{12}-1)\Delta I = \frac{1}{(1+\varepsilon_1)^{(2n_{12}-1)}} \qquad (19)$$

is satisfied.

Calculation of the burst time is carried out in finite steps from the initial strain value of $\varepsilon_1 = 0$. After determination of the material properties, pressure and temperature for the next time step, ΔI is calculated from equation (17). Using the old strain ε_1, a new value ε_2 is calculated using equation (18). The two sides of equation (19) are then compared to ensure that the right-hand side of the equation is smaller than or equal to the left-hand side. If this is the case, burst time has been reached. Otherwise, the calculation is repeated using the new strain value until condition (19) is satisfied. The burst pressure and burst temperature are also known at that stage, and the burst stress and burst strain can be calculated from equations (6) and (7), respectively.

3. MATERIAL PROPERTIES

3.1 STEADY-STATE CREEP RATES

3.1.1 Steady-State Creep Rates of Zircaloy-4 in the α-Region

For Zircaloy-4 containing 0.10 and 0.16 wt.% oxygen, the hexagonal-close-packed α-Zr phase extends to temperatures of ∿ 1085 K. Uniaxial creep tests on recrystallized Zircaloy-4 have been reported by Rosinger et al.[11]. Additional steady-state creep data have since been generated at 823 K, 873 K and 923 K. The Norton creep equation, equation (1), was fitted to all the experimental data, including those of Clendening[10] and Busby and Marsh[12], to obtain the best-fit numerical values of A, n and Q. These are listed in Table 1. In agreement with others[11,12-18], the values of A, n and Q are constant from 823 K to 1073 K.

3.1.2 Steady-State Creep of Zircaloy-4 in the β-Region

For Zircaloy-4 containing 0.10 and 0.16 wt.% oxygen, the body-centered-cubic β-Zr phase extends from 1248 K to the melting point of ∿ 2125 K. The creep data for Zircaloy-4 in the 1273 K to 1873 K temperature range are given by Rosinger et al.[11], Rizkalla et al.[19] and Busby and White[20]. The values of A, n and Q for the β-Zr phase are given in Table 1. These values are constant[11,15,19-22] over the complete temperature range.

3.1.3 Steady-State Creep of Zircaloy-4 in the α+β Region

For Zircaloy-4 containing 0.10 to 0.16 wt.% oxygen, the α+β region, which contains both the hexagonal-close-packed α-Zr phase and the body-centered-cubic β-Zr phase, extends from 1085 K to 1248 K.

The steady-state creep of the α+β region is relatively unknown. Chung et al.[23], Garde et al.[24], Bocek et al.[25] and Rosinger et al.[11] have found a low stress exponent of about two at low creep rates. Combining the Zircaloy-4 data by Clendening[10] and Rosinger et al.[11] with the Zircaloy-2 data by Rose and Hindle[15] and Clay and Redding[18] yields, for the low creep region, i.e., $\dot{\varepsilon} \leq 3 \times 10^{-3}\ s^{-1}$, the values of A, n and Q given in Table 1. At higher creep rates, the stress exponent appears to increase.

Because of the great differences in stress exponent and activation energy in the α+β phase region compared to those in the α-Zr and β-Zr phase regions, certain assumptions must be made. Healey et al.[26] overcame the lack of creep data for the α+β region by assuming that the transition from α-Zr to β-Zr occurred at 1198 K for a heating rate of 25 $K \cdot s^{-1}$ and at 1223 K for 100 $K \cdot s^{-1}$.

In this work, two cases are considered:

(i) $\dot{\varepsilon} \leq 3 \times 10^{-3}\ s^{-1}$

It is assumed that n and Q vary linearly from the values at the α/α+β transus temperature to their respective values at the mid-temperature of the α+β phase region and from those linearly to their respective values at the α+β/β transus temperature.

The value of A is logarithmically varied from the value at the α/α+β transus temperature to the value at the mid-temperature of the α+β region and from that to the value at the α+β/β transus temperature.

(ii) $\dot{\varepsilon} > 3 \times 10^{-3}\ s^{-1}$

For $\dot{\varepsilon} > 3 \times 10^{-3}\ s^{-1}$ the stress exponent is expected to be significantly larger than the value of 2.33 given in Table 1. Because

of a lack of data, however, its exact value is not known. Consequently, it is assumed that n and Q vary linearly with temperature between the $\alpha/\alpha+\beta$ and the $\alpha+\beta/\beta$ transus temperatures. The value of A is allowed to vary logarithmically over the same temperature range.

Using the above values of A, n and Q, modified by equation (15) with F = G = H = 0.5, the burst temperature was calculated as a function of the initial stress and heating rate. The calculations were performed for constant heating rates and constant internal pressures. The results, plotted in Figure 2, show that the burst temperature increases with decreasing initial stress and is a function of the heating rate. Increasing the heating rate at the same initial stress significantly increases the burst temperature.

3.2 EFFECT OF MULTIAXIAL STRESS STATE AND ANISOTROPY

In Section 2.2 we showed that the parameter A of the creep equations must be modified because the diametral strain rates in tubes are calculated. Equations (13) and (15) are combined to yield the tangential (diametral) strain rate $\dot{\varepsilon}_\theta$ as:

$$\dot{\varepsilon}_\theta = A_z \cdot \frac{\left(\frac{F+G}{4}+H\right)^{(n-1)/2} \cdot (H+0.5F)}{(F+G)^{(n+1)/2}} \cdot \sigma_\theta^{\,n} \cdot \exp\left(\frac{-Q}{kT}\right) \qquad (20)$$

If the material is isotropic then, according to Ross-Ross et al.[8], F = G = H = 0.5 and equation (20) changes to:

$$\dot{\varepsilon}_\theta = A_z \cdot (0.866)^{n+1} \cdot \sigma_\theta^{\,n} \cdot \exp\left(\frac{-Q}{kT}\right) \qquad (21)$$

Work by Hunt[6], however, has shown that the α-Zr phase of Zircaloy-4 is not isotropic. Only in the α+β region do the anisotropic factors change from anisotropic to isotropic.

For the calculations performed in this work it is assumed that only the α-Zr phase is anisotropic and that the α+β and β-Zr phases are isotropic.

The influence of anisotropy on the burst data is shown in Figure 3. The anisotropic factors of Hunt[6] and Rosinger et al.[27] were employed. It can be seen that the degree of anisotropy has a considerable effect on the absolute value of the burst temperature. For example, at 70 MPa, the burst temperature is raised by over 70 K between the isotropic case and the most severe anisotropy.

4. COMPARISON OF THEORY AND EXPERIMENT

Using the anisotropic factors of F = 0.934, G = 0.374 and H = 0.192, the theoretical burst temperature as a function of the initial stress for heating rates of 0.5, 1, 5, 10, 30 and 100 $K \cdot s^{-1}$ was calculated. The results are shown in Figure 4. In general appearance the curves are similar to those shown in Figure 2 except that they are somewhat higher. Again, the burst temperature of the cladding increases with heating rate.

The effect of heating rate on the burst temperature of Zircaloy cladding, deforming under the influence of a constant differential pressure in an inert or vacuum atmosphere, has been investigated by several authors[28-32]. The results of such experiments for heating rates from 15 to 40 $K \cdot s^{-1}$ are shown in Figure 5 and compared with the calculated burst temperature. The identification of the plotting symbols is

found in Table 2 where the test conditions are also listed. The agreement in Figure 5 between experiment and theory is excellent.

Several authors[33-36] have investigated the deformation of closed Zircaloy cladding under the influence of a slightly variable pressure in an inert atmosphere or vacuum. Usually the clad tubing was pressurized in the 575 to 625 K range. The pressure was then isolated and allowed to vary as the cladding was heated up, allowed to strain and finally to rupture. A comparison of the data for constant pressure tests from Figure 5 with the data for closed tubes when the pressure varied slightly during the temperature ramp is shown in Figure 6. No significant difference is noted for the two pressure conditions. It is, consequently, possible to calculate the burst temperature for the slightly variable pressure observed in closed tubes using the assumption that the pressure is constant throughout the temperature range.

In addition, a series of burst tests was performed in a steam or oxygen atmosphere at either constant[29,30,37] or slightly variable differential pressure (closed tubes)[35,36,38,39]. Figure 7 is a plot of these data for heating rates from 15 to 40 $K \cdot s^{-1}$ and the data from Figure 6. In the α-region, i.e., $T < 1250$ K, no significant difference is noted for the two atmospheric conditions, inert atmosphere or vacuum versus oxidizing atmosphere, i.e., the atmosphere has no apparent effect on the burst temperature. Again the agreement between experimental and theoretical burst temperature is excellent.

For LOCA application, the correlation between burst temperature and burst stress for irradiated cladding is of particular importance. As seen in Figure 7, there is no difference between the irradiated cladding of Karb[39] and the unirradiated cladding.

Figures 8 and 9 include the burst temperature data for all the test conditions given in Table 2 for heating rates from 0.7 to 3.0 $K \cdot s^{-1}$ and from 70 to 250 $K \cdot s^{-1}$, respectively. Both figures show excellent

agreement between experiment and theory. Therefore, the theory can be used to calculate successfully the burst temperature as a function of the initial stress and heating rate.

Brzoska et al.[5] have developed a relationship (equation (6)) between burst stress and burst temperature which is used in this work to calculate the burst strain in accordance with equation (7). For our current values of a and b, the relationship between the burst strain and the burst temperature with heating rate is shown in Figure 10. The figure demonstrates that the burst strain is heating rate dependent and has a dip in the $\alpha+\beta$ region. This is observed experimentally[35].

For comparison, some of the newest experimental data by Schmidt[37] are also shown in Figure 10. These data, currently being generated in a test facility[40] which minimizes the azimuthal temperature gradients, will eventually be used to calculate the proper values of a and b in equation (6).

Figure 11 shows the relationship between the burst strain and the burst temperature for heating rates from 15 to 40 $K \cdot s^{-1}$. The dramatic extremes in the experimental data for burst strain by various authors help to point out the difficulty in obtaining a proper burst strain correlation. The theoretical curve, calculated for a heating rate of 25 $K \cdot s^{-1}$, follows, in general, the experimental data.

5. DISCUSSION

The model presented is used to predict the burst temperature and burst strain of a cladding subjected to constant differential pressures and constant heating rates. There are, of course, deviations between the experimental data and the calculated values. This is to be expected and can be traced to numerous causes which are examined below.

Burst data in the literature are usually reported for constant heating rates. In actual fact, however, the heating rate can vary and, since both the burst temperature and the burst strain are functions of the heating rate, any variation in the heating rate within a particular set of experiments will influence these two properties. Chung and Kassner[35], for example, report a heating rate from their starting temperature to 1073 K range. They do not report the heating rate above that temperature. This is unfortunate since the heating rate over the last 50 to 100 K before the burst has a controlling influence on the burst temperature and, especially, the burst strain. Since the heating rate for a constant power input usually decreases with increasing temperature, it is expected that the experimental burst temperature will be lower and the experimental burst strain will be higher than are predicted by the model. Figures 6 to 9 show that the experimental burst temperature is lower than the calculated burst temperature.

The burst data can also be influenced if the pressure is not constant during the experiment. Many of the authors have reported only a starting differential pressure at a particular temperature. It is known, however, that the pressure in a closed tube increases with temperature. As the temperature is raised, the pressure increases and this strains the cladding which deforms causing a decrease in pressure. Using the proposed model, the effect of time-dependent pressure and heating rate can be calculated.

Work by Erbacher et al.[41] has shown that severe azimuthal temperature differences can be obtained around the circumference of the cladding during a test. These azimuthal temperature differences have a great effect on the experimentally determined strains. Erbacher et al. have shown that large azimuthal temperature differences result in a small burst strain, while small azimuthal temperature differences result in significantly larger and more uniform burst strains.

Unless the exact burst position on the cladding is known, it is difficult to measure the exact burst temperature. Any measuring position not directly located on the burst will result in lower reported burst temperatures. This is another reason why the experimental burst temperatures are invariably below the calculated burst temperatures, as seen in Figures 6 to 9.

In Section 3.2 it was shown that the anisotropy of the Zircaloy can significantly change the burst temperature in the α-Zr region. Unfortunately, knowledge of the anisotropic factors is very limited[6]. In this work we arbitrarily chose the values of F = 0.924, G = 0.374 and H = 0.192 for the anisotropic factors.

In developing the burst criterion model, it was assumed that the burst data could be calculated from the steady-state creep equation. This assumption is justified at low strain, but its application is doubtful when the burst strain is approached. Near the burst strain, plastic instabilities and tertiary creep - both unknown - should probably be considered.

In addition, the values of A, n and Q for steady-state creep are not sufficiently well known for the α+β region. An experimental program is, however, under way to determine these values.

In spite of the above limitations, the burst criterion model developed in this work has been applied successfully to calculate the burst temperature. The verification of the burst strain portion of the model requires careful experimental determination of the burst strain when no azimuthal temperature differences are present.

6. CONCLUSIONS

In this work, a burst criterion model which assumes that the deformation is controlled by the steady-state creep of the material has been developed for thin-walled cladding subjected to a differential pressure. The creep equation is integrated to obtain a burst time at the singularity of the strain. Once the burst time is known, the burst temperature and the burst pressure can be calculated from the known temperature and pressure histories. A further empirical relationship between burst stress and burst temperature is used to calculate the burst strain. Within the scope of the present work, which assumes a constant pressure history, the following conclusions are made:

1. If the heating rate is constant, the burst temperature increases with decreasing initial stress.

2. If the stress level is constant, the burst temperature increases with increasing heating rate.

3. Anisotropy in the α-Zr range significantly alters the burst temperature.

4. The calculated burst strain, in agreement with experiment, has a dip in the $\alpha+\beta$ region.

5. If the burst temperature is constant, the burst strain increases with decreasing heating rate.

6. For the same nominal test conditions and burst temperatures, there is an extremely wide variation of burst strains reported in the literature.

7. The differences between theory and experiment can be attributed to the following: heating rate not constant during the test, pressure not constant during the test, azimuthal tem-

perature differences, burst temperature not measured at the burst location, anisotropy, the use of steady-state creep equation to failure, and a lack of knowledge of creep in the $\alpha+\beta$ phase region. The burst data calculated from the developed model are, nevertheless, in good agreement with the experimental data.

REFERENCES

1. W. Gulden, "SSYST-1. A Computer Code System to Analyse the Fuel Rod Behaviour During a Loss-of-Coolant Accident", KFK-2496 (1977).

2. L.J. Sieken, "FRAP-T4 -- A Computer Code for the Transient Analysis of Oxide Fuel Rods", EG&G Idaho, Inc. Report CDAP-TR-78-027 (1978).

3. J.J.M. Too and H. Tamm, "FAXMOD and Its Application to the Prediction of High Temperature Creep and Sheath Ballooning Behaviour", Nuc. Eng. Des. (in press).

4. S. Banerjee, H.J. Bridges and J.J.M. Too, "A Model for Analysis of Fuel Behaviour in Transients", Nucl. Eng. Des. 42, 319 (1977).

5. B. Brzoska, G. Cheliotis, A Kunick and G. Senski, "A New High-Temperature Deformation Model for Zircaloy Clad Ballooning Under Hypothetical LOCA Conditions", Trans. 4th Int. Conf. Structural Mechanics in Reactor Technology, C 1/8, San Francisco (1977).

6. C.E.L. Hunt, "Anisotropy Theory and the Measurement and Use of Anisotropic Factors for Zircaloy-4 Fuel Sheaths", Trans. 4th Int. Conf. Structural Mechanics in Reactor Technology, C 2/9, San Francisco (1977).

7. G.E. Lukas and A.L. Bement, "The Effect of Zirconium Differential on Cladding Collapse Predictions", J. Nucl. Mater. 55, 246 (1975).

8. P.A. Ross-Ross, V. Fidleris and D.E. Fraser, "Anisotropic Creep Behaviour of Zirconium Alloys in a Fast Neutron Flux", Can. Met. Quart. 11, 101 (1972).

9. R. Hill, "A Theory of the Yielding and Plastic Flow of Anisotropic Metals", Proc. Roy. Soc. A 193, 281 (1948).

10. W.R. Clendening, "Primary and Secondary Creep Properties for Zircaloy Cladding at Elevated Temperatures in Accident Analysis", 3rd Structural Materials in Reactor Technology Conf., London, England (1975).

11. H.E. Rosinger, P.C. Bera and W.R. Clendening, "The Steady-State Creep of Zircaloy-4 Fuel Cladding from 940 to 1873 K", Atomic Energy of Canada Limited Report, AECL-6193 (1978) and J. Nucl. Mater. 82, 286 (1979).

12. C.C. Busby and K.B. Marsh, "High Temperature, Time-Dependent Deformation in Internally Pressurized Zircaloy-4 Tubing", Westinghouse Electric Corp., Bettis Atomic Power Laboratory Report, WAPD-TM-1043 (1974).

13. E.D. Hindle, "Creep and Mechanical Properties of Zircaloy Fuel Element Cladding in Steam", presentation at the 3rd Water Reactor Safety Research Information Meeting, Gaithersburg, Md., U.S.A., 1975.

14. J.J. Holmes, "The Activation Energy for Creep of Zircaloy-2", J. Nucl. Mater. 13, 137 (1964).

15. K.M. Rose and E.D. Hindle, "Diameter Increases in Steam Generating Heavy Water Reactor Zircaloy Cans Under Loss-of-Coolant Accident Conditions" in Zirconium in the Nuclear Industry; Proceedings, A.L. Lowe and G.W. Parry, editors, ASTM STP 633, 24 (1977).

16. I.M. Bernstein, "Diffusion Creep in Zirconium and Certain Zirconium Alloys", Trans. TMS-AIME 239, 1518 (1967).

17. B.D. Clay and G.B. Redding, "Creep Rupture Properties of Alpha-Phase Zircaloy Cladding Relevant to the LOCA", J. BNES 15, 253 (1976).

18. B.D. Clay and G.B. Redding, "Creep Rupture Properties of Alpha-Phase Zircaloy-2 Cladding Relevant to the Loss-of-Coolant Accident", Central Electricity Generating Board Report, CEGB RD/B/N-3187 (1975).

19. A.S. Rizkalla, R.A. Holt and J.J. Jonas, "The Effect of Oxygen on the Deformation of Zircaloy-4 at Elevated Temperatures", 4th Int. Conf. on Zirconium in the Nuclear Industry, Stratford, England (1978).

20. C.C. Busby and L.S. White, "Some High Temperature Mechanical Properties of Internally Pressurized Zircaloy-4 Tubing", Westinghouse Electric Corp., Bettis Atomic Power Laboratory Report, WAPD-TM-1243 (1976).

21. B. Burton, G.L. Reynolds and J.P. Barnes, "Tensile Creep of Beta-Phase Zircaloy-2", Central Electricity Generating Board Report, CEGB RD/B/N-4073 (1977) and J. Nucl. Mater. 73, 70 (1978).

22. B.D. Clay and R. Stride, "The Primary and Secondary Creep Properties of Beta-Phase Zircaloy-2 in the Region 1200° to 1500°C", Central Electricity Generating Board Report, CEGB RD/B/N-3950 (1977).

23. H.M. Chung, A.M. Garde and T.F. Kassner, "Mechanical Properties of Zircaloy Containing Oxygen", Argonne National Laboratory Report, ANL-76-121 (1976).

24. A.M. Garde, H.M. Chung and T.F. Kassner, "Micrograin Superplasticity in Zircaloy at 850°C", Acta Met. 26, 153 (1978).

25. M. Bocek, G. Faisst and C. Petersen, "Examination of the Plastic Properties of Zircaloy-4 at Elevated Temperatures in Air Atmosphere", J. Nucl. Mater. 62, 26 (1976).

26. T. Healey, H.E. Evans and R.B. Duffey, "Deformation and Rupture of Pressurized and Transiently Heated Zircaloy Tube", J. BNES 15, 247 (1976).

27. H.E. Rosinger, J. Bowden and R.S.W. Shewfelt, "Zircaloy-4 Fuel Cladding Anisotropy at 1073 K", Atomic Energy of Canada Limited Report, AECL-6447, in preparation.

28. D.G. Hardy, "High Temperature Expansion and Rupture Behaviour of Zircaloy Tubing", ANS Topical Meeting on Water Reactor Safety, Salt Lake City, Utah (1973), conf. paper CONF-730304.

29. E.F. Juenke and J.F. White, "Physical-Chemical Studies of Clad UO_2 Under Reactor Accident Conditions", General Electric Co. Report, GEMP-731 (1970).

30. K.M. Emmerich, E.F. Juenke and J.F. White, "Failure of Pressurized Zircaloy Tubes during Thermal Excursions in Steam and Inert Atmospheres", Symposium on Applications Related Phenomena in Zirconium and its Alloys, ASTM STP 458, 252 (1969).

31. P. Morize, H. Vidal, J.M. Frenkel and R. Roulliay, "Zircaloy Cladding Diametral Expansion during a LOCA", CSNI Specialist Meeting on the Behavior of Water Reactor Fuel Elements under Accident Conditions, Spaatind, Norway (1976).

32. C.E.L. Hunt and W.G. Newell, "The Ballooning Behaviour of Zircaloy-4 Fuel Sheaths at a Heating Rate of 0.5°C/s", Atomic Energy of Canada Limited Report, AECL-6342 (1978).

33. D.O. Hobson, M.F. Osborne and G.W. Parker, "Comparison of Rupture Data from Irradiated Fuel Rods and Unirradiated Cladding", Nucl. Technology 11, 479 (1971).

34. B.D. Clay, T. Healey and G.B. Redding, "The Deformation and Rupture of Zircaloy-2 Tubes During Transient Heating", Central Electricity Generating Board Report, CEGB RD/B/N-3512 (1976).

35. H.M. Chung and T.F. Kassner, "Deformation Characteristics of Zircaloy Cladding in Vacuum and Steam Under Transient-Heating Conditions: Summary Report", Argonne National Laboratory Report, ANL-77-31 (1978).

36. C.L. Mohr, "Transient Deformation Properties of Zircaloy for LOCA Simulation", Electric Power Research Institute Report, EPRI NP-526 (1978).

37. H. Schmidt, KFK, IRB, private communition (1979).

38. R.H. Chapman, "Preliminary Multirod Burst Test Program Results and Implications of Interest to Reactor Safety Evaluations", presentation at the 6th Water Reactor Safety Research Information Meeting, Gaithersburg, Md., U.S.A., 1978.

39. E.H. Karb, "Results of the FR2 Nuclear Tests on the Behaviour of Zircaloy Clad Fuel Rods", presentation at the 6th Water Reactor Safety Research Information Meeting, Gaithersburg, Md., U.S.A., 1978.

40. K. Wiehr and H. Schmidt, "Out-of-Pile Experiments on Ballooning of Zircaloy Fuel Rod Claddings. Test Results with Shortened Fuel Rod Simulators", KFK-2345 (1977).

41. F. Erbacher, H.J. Neitzel and K. Wiehr, "Interaction Between Thermohydraulics and Fuel Clad Ballooning in a LOCA; Results of REBEKA Multirod Bundle Tests with Flooding", presentation at the 6th Water Reactor Safety Research Information Meeting, Gaithersburg, Md., U.S.A., 1978.

TABLE 1

VALUES OF A, n AND Q FOR THE EQUATION

$$\dot{\varepsilon} = A\sigma^{n} \cdot \exp\,[-Q(kT)^{-1}]$$

AS DETERMINED FROM UNIAXIAL CREEP TESTS

Phase	A $(MPa)^{-n} \cdot s^{-1}$	n	Q $J \cdot mol^{-1}$	T K
α-Zr	1.937×10^{4}	5.89	320 200	823-1085
(α+β)-Zr	0.24*	2.33*	102 400*	1166.5*
β-Zr	7.9	3.78	142 000	1248-1873

* Values for $\dot{\varepsilon} \leq 3 \times 10^{-3} \cdot s^{-1}$

TABLE 2

COMPILATION OF BURST DATA

Plotting Symbols	Pressure	Atmosphere	Heating Rates $K \cdot s^{-1}$	References
■	constant	vacuum	0.5 to 100	Hardy[28]
▲	constant	inert	0.18 to 125	Juenke & White[29], Emmerich, Juenke & White[30]
●	constant	vacuum	5 to 50	Morize et al.[31]
◆	constant	vacuum	0.5	Hunt & Newell[32]
⯭	closed tube	inert	5.5 to 55.6	Hobson, Osborne & Parker[33]
⯭	closed tube	inert	5.0 to 17.2	Hobson et al.[33], irradiated clad
+	closed tube	inert	0.3 to 50	Clay, Healey & Redding[34]
⧗	closed tube	vacuum	3.5 to 140	Chung & Kassner[35]
⌘	closed tube	vacuum	0.9 to 74	Mohr[36]
△	closed tube	steam	0.1 to 240	Juenke & White[29], Emmerich, Juenke & White[30]
⏱	constant	steam	1, 10, 30	Schmidt[37]
◈	closed tube	steam	4.0 to 129	Chung & Kassner[35]
X	closed tube	steam	4.0 to 28	Chapman[38]
⧗	closed tube	1 atm. 80% Ar + 20% O_2	0.9 to 56	Mohr[36]
✱	closed tube	steam	5.5 to 19.4	Karb[39], irradiated clad

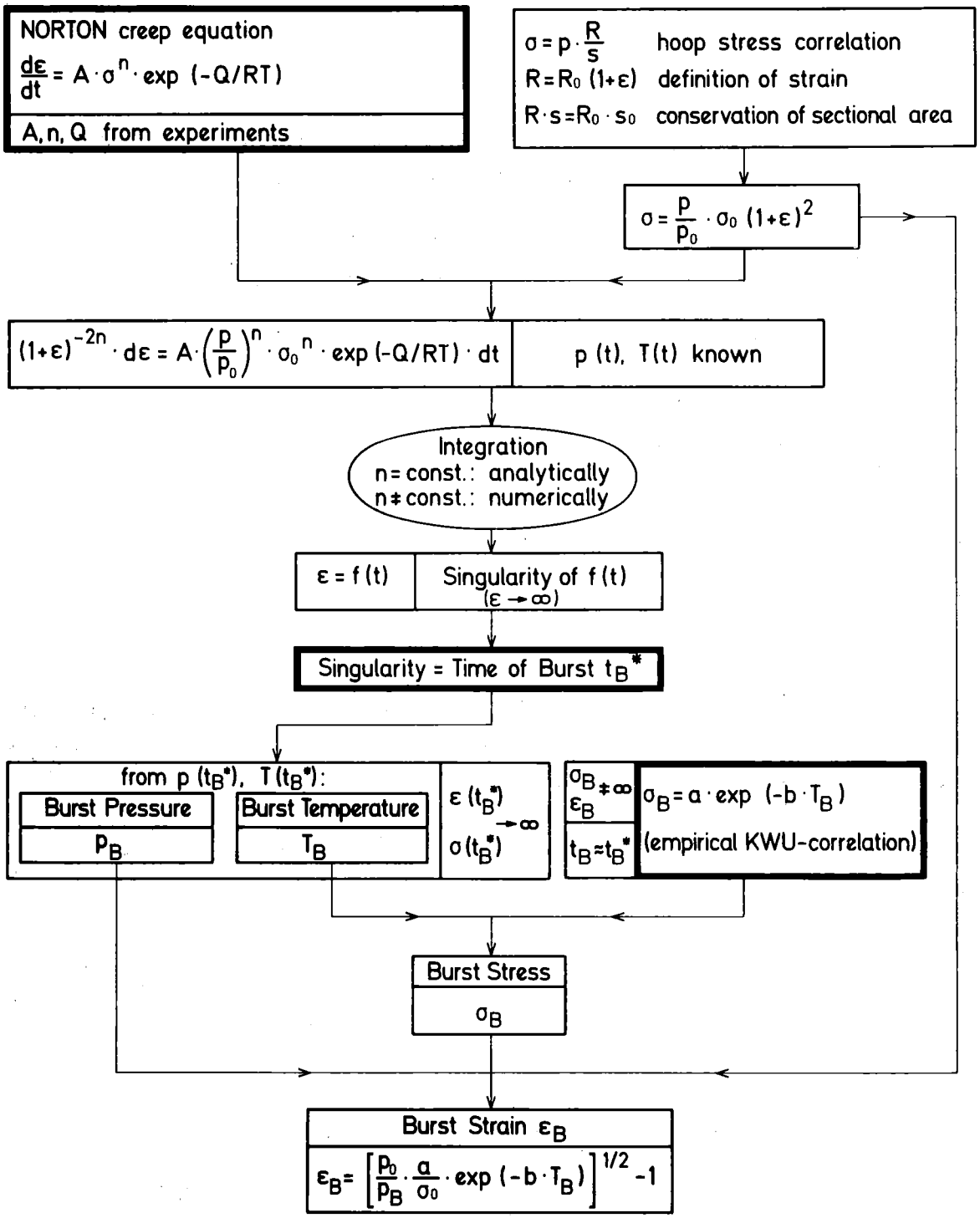

FIGURE 1: Development of a Burst Criterion

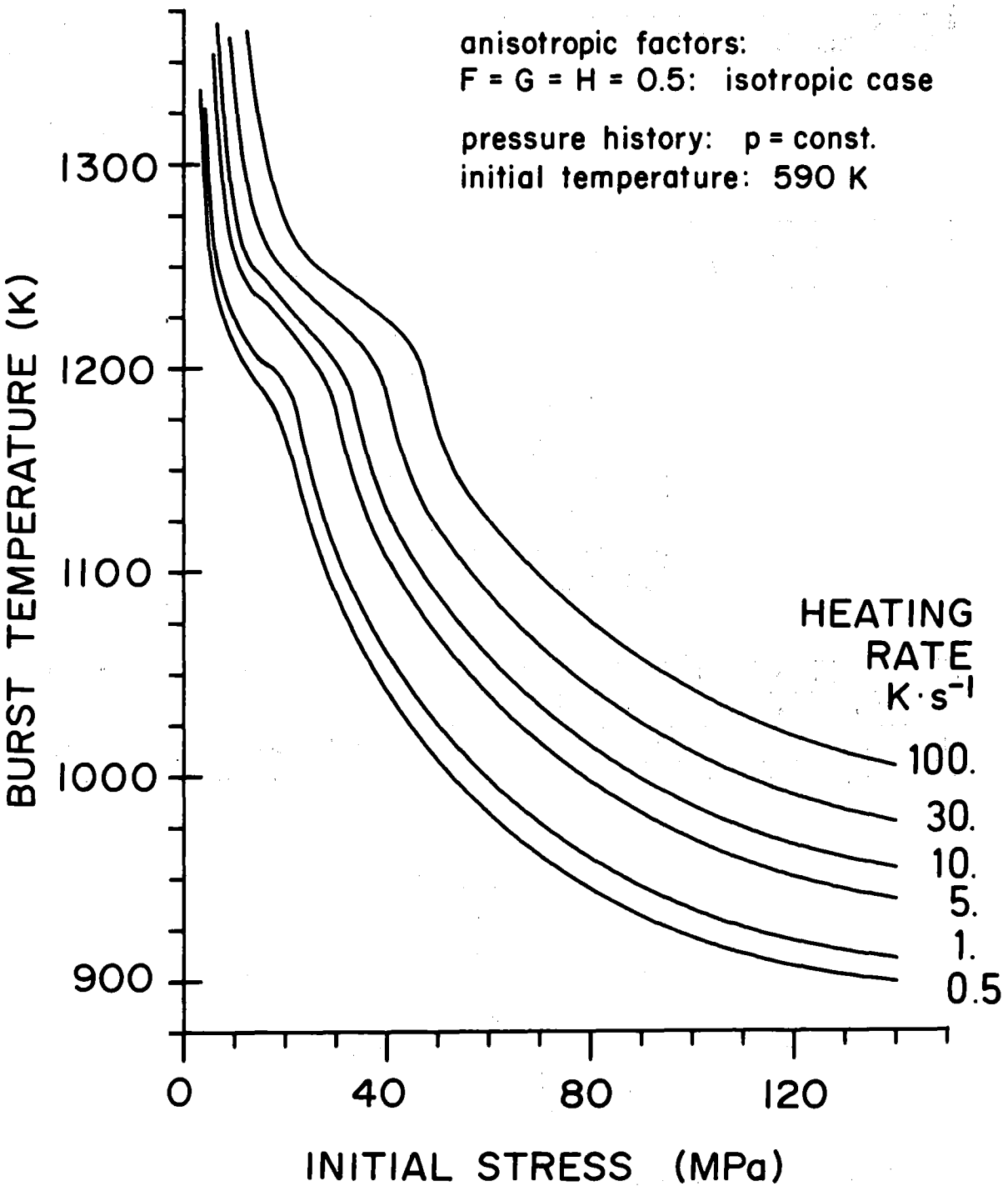

FIGURE 2: Relationship between Burst Temperature and Initial Stress for Various Heating Rates.

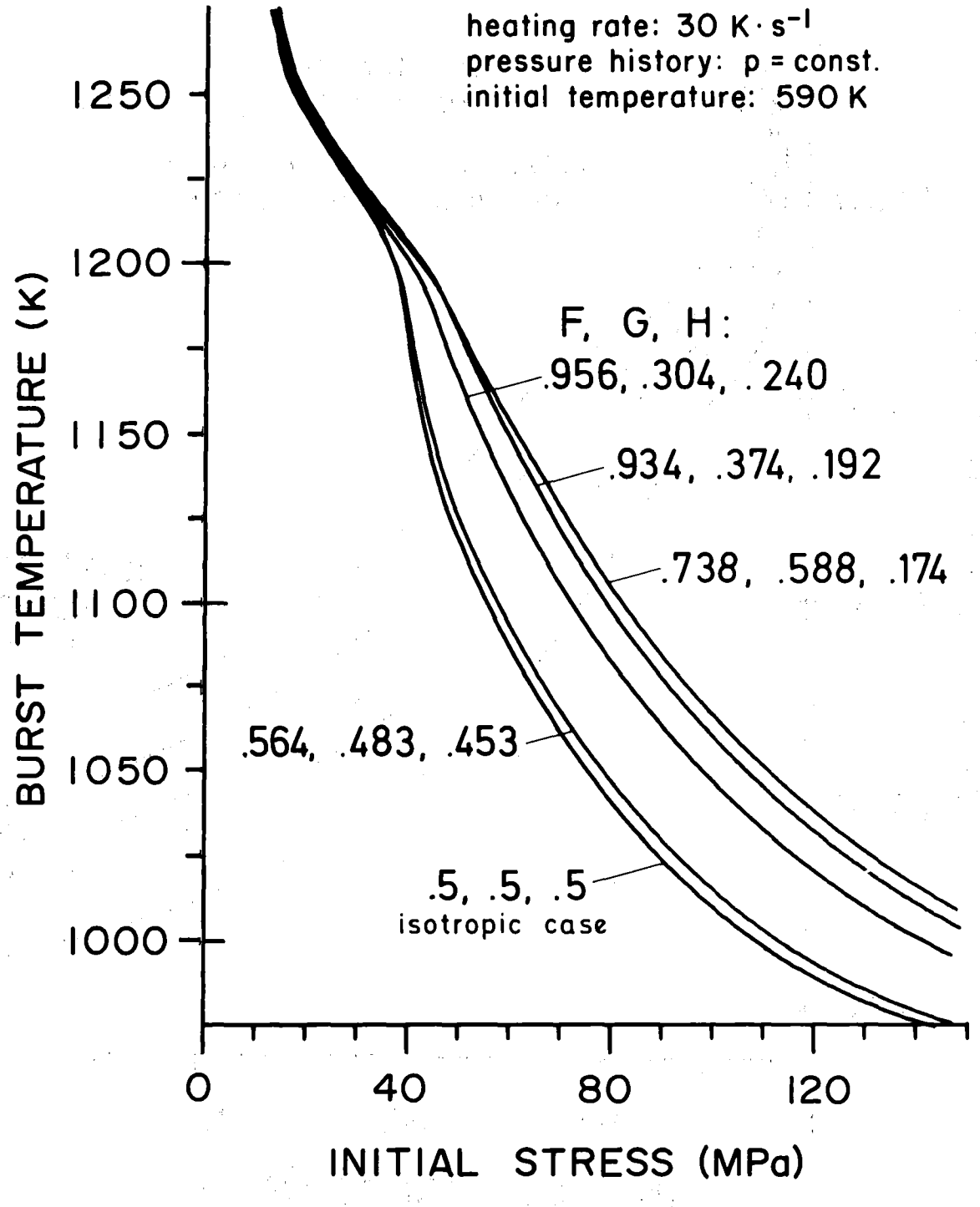

FIGURE 3: Influence of Anisotropy on the Relationship between Burst Temperature and Initial Stress

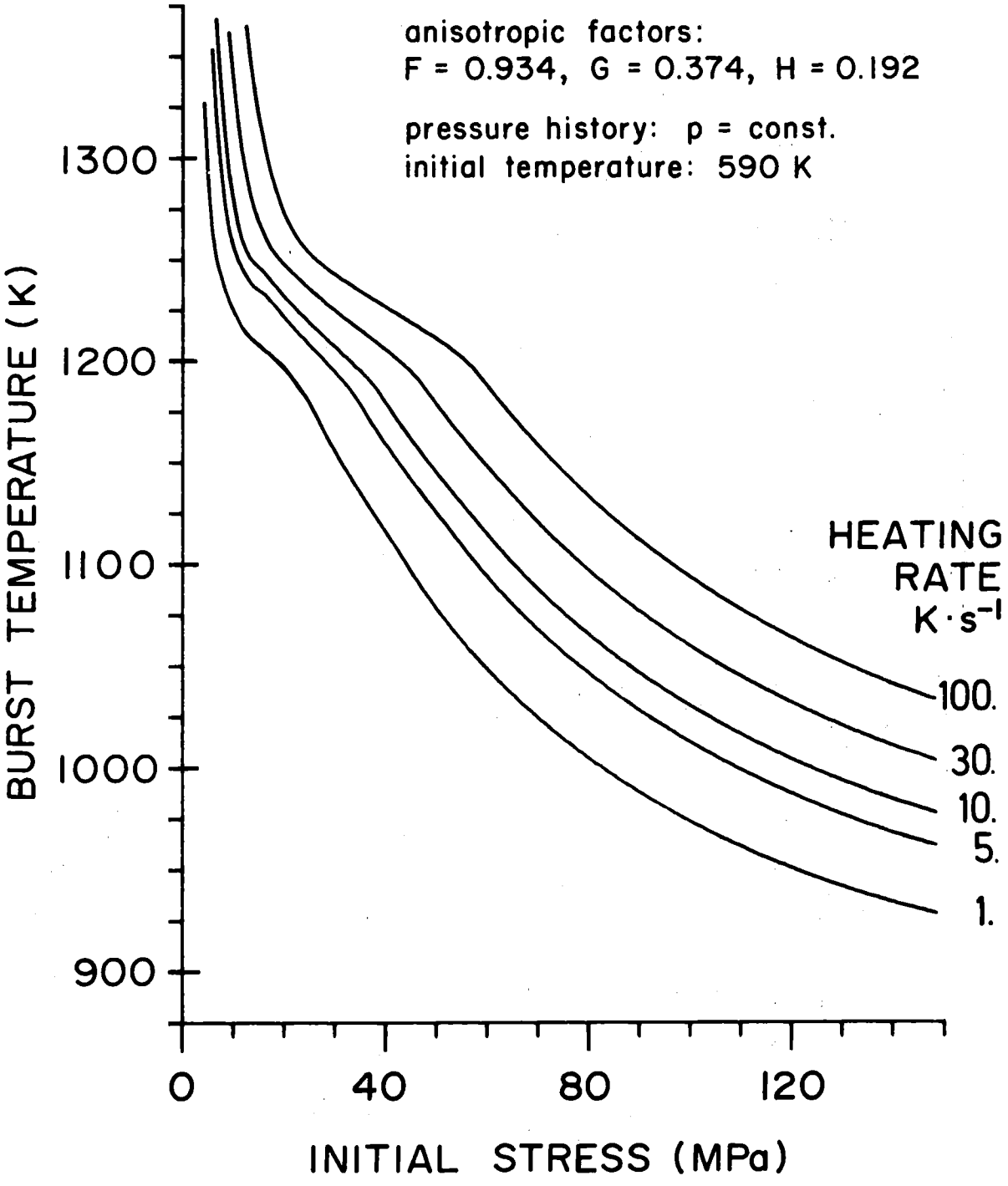

FIGURE 4: Relationship between Burst Temperature and Initial Stress for Various Heating Rates

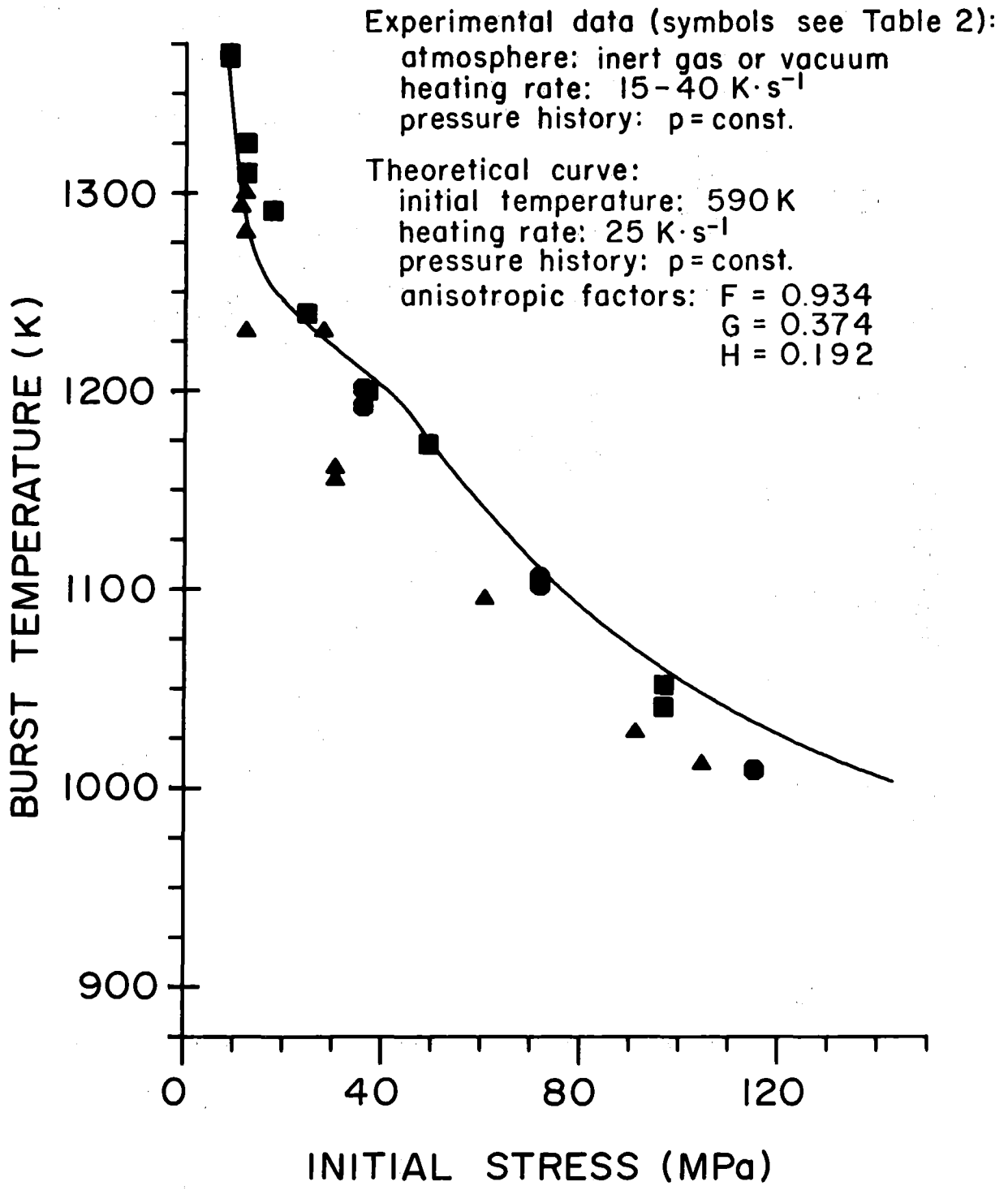

FIGURE 5: Comparison of Experimental Data with Theoretical Curve for Burst Temperature versus Initial Stress

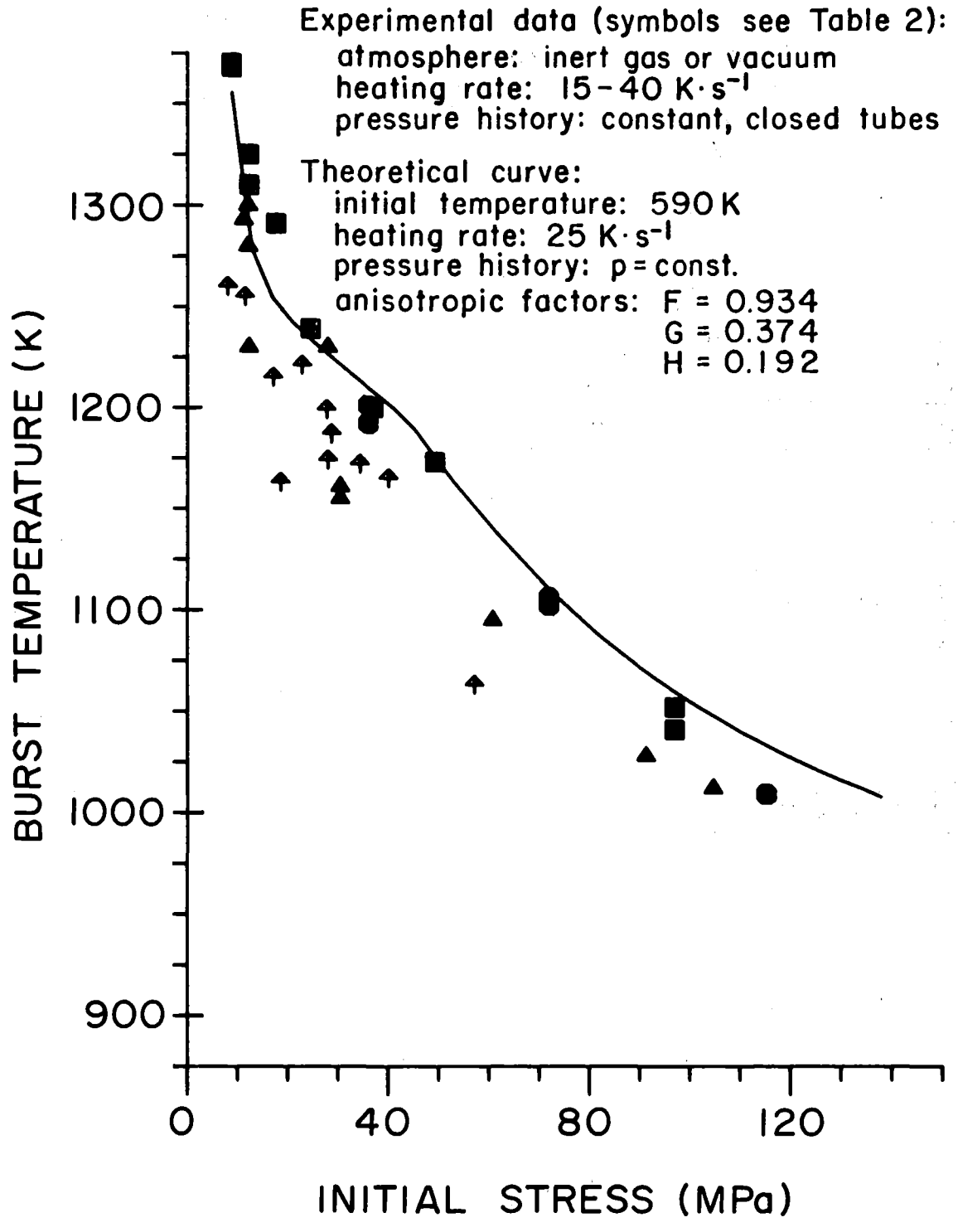

FIGURE 6: Comparison of Experimental Data with Theoretical Curve for Burst Temperature versus Initial Stress

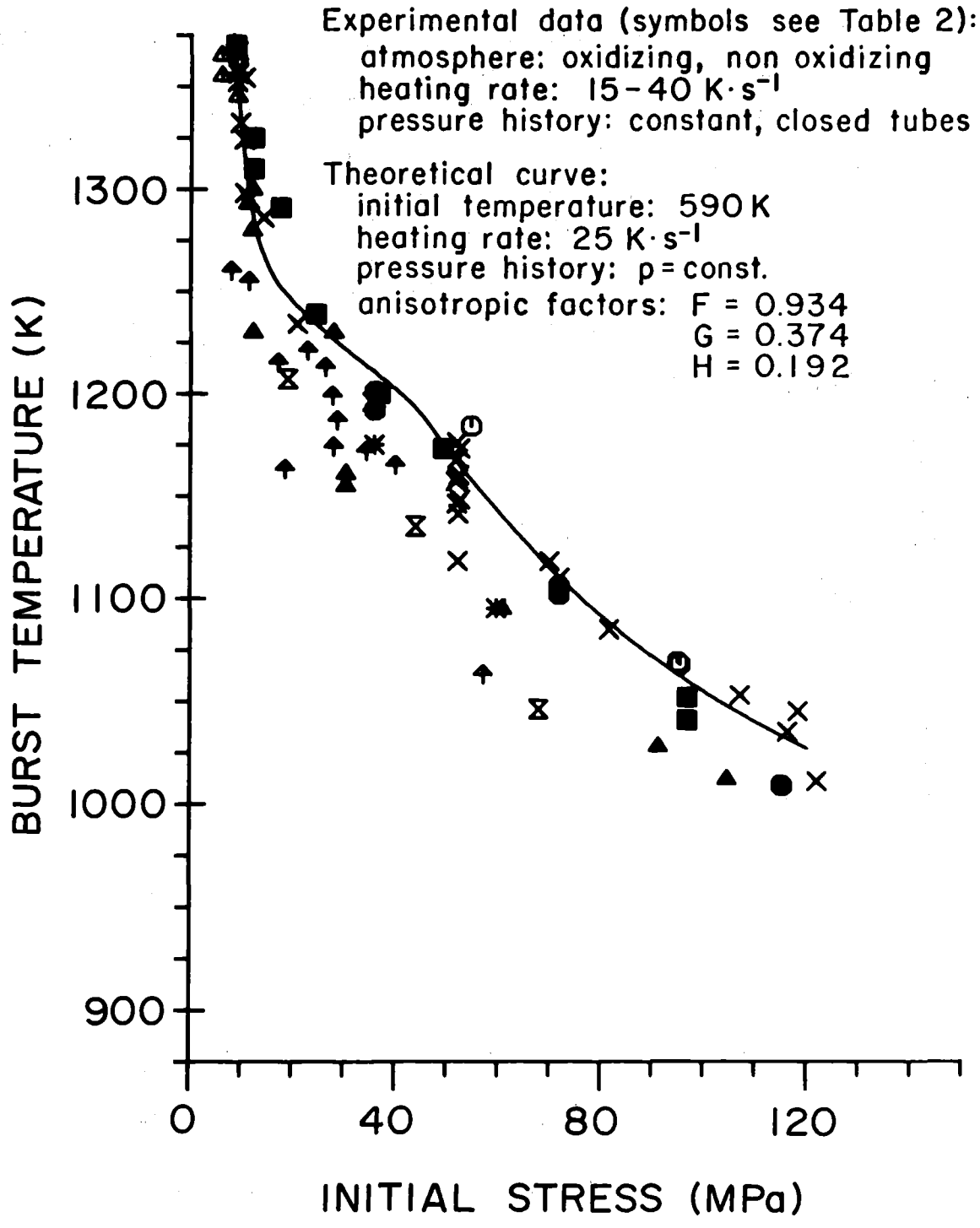

FIGURE 7: Comparison of Experimental Data with Theoretical Curve for Burst Temperature versus Initial Stress

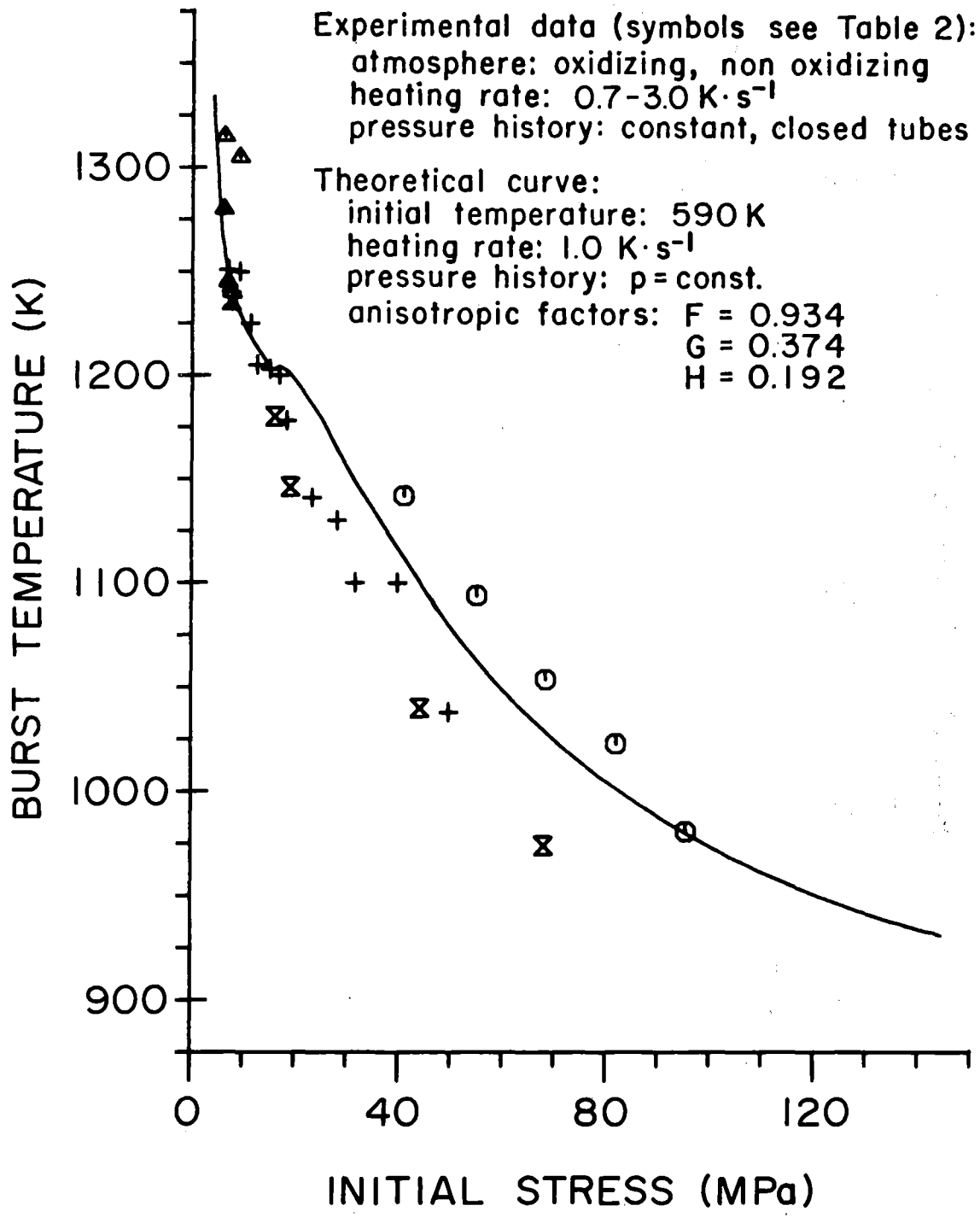

FIGURE 8: Comparison of Experimental Data with Theoretical Curve for Burst Temperature versus Initial Stress

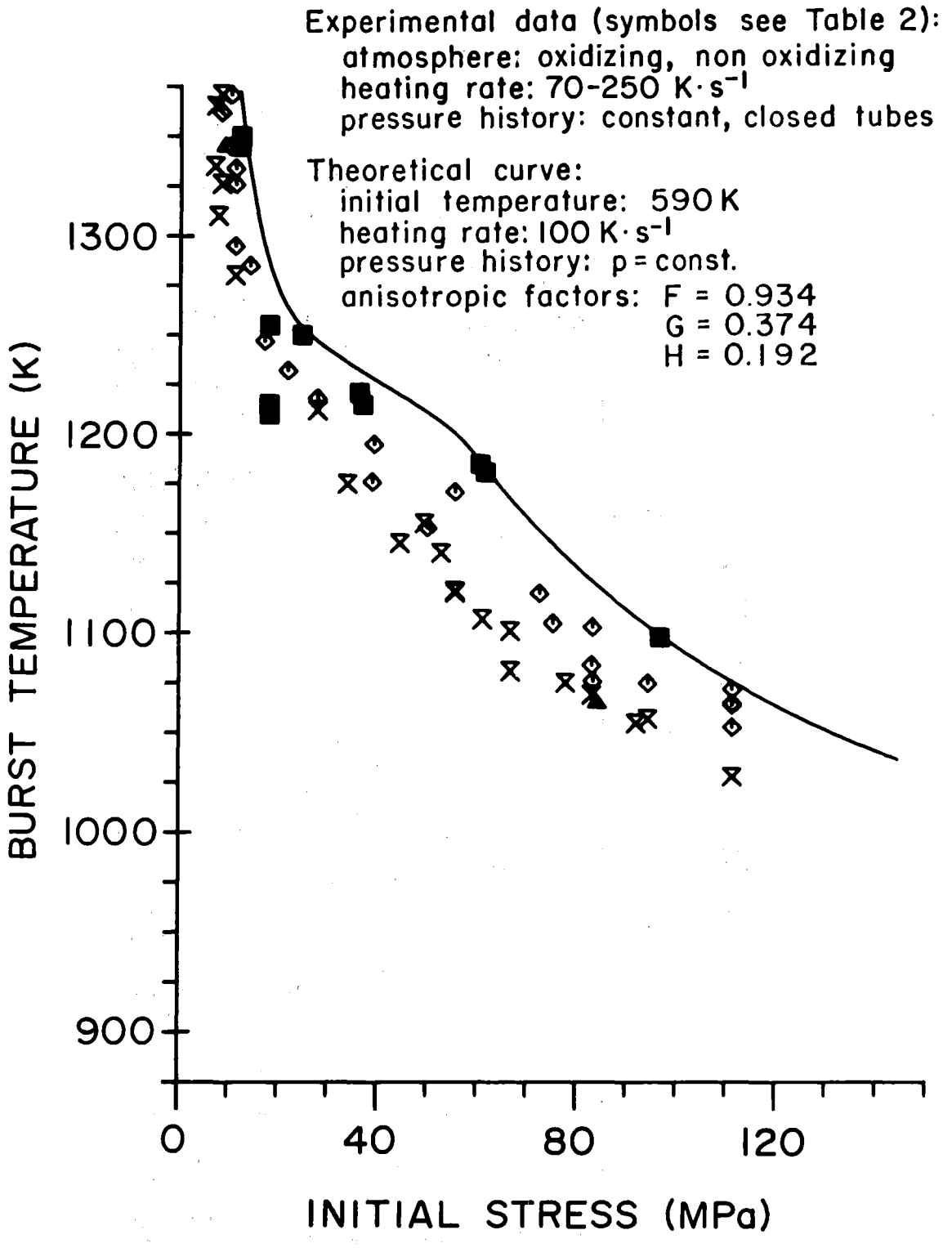

FIGURE 9: Comparison of Experimental Data with Theoretical Curve for Burst Temperature versus Initial Stress

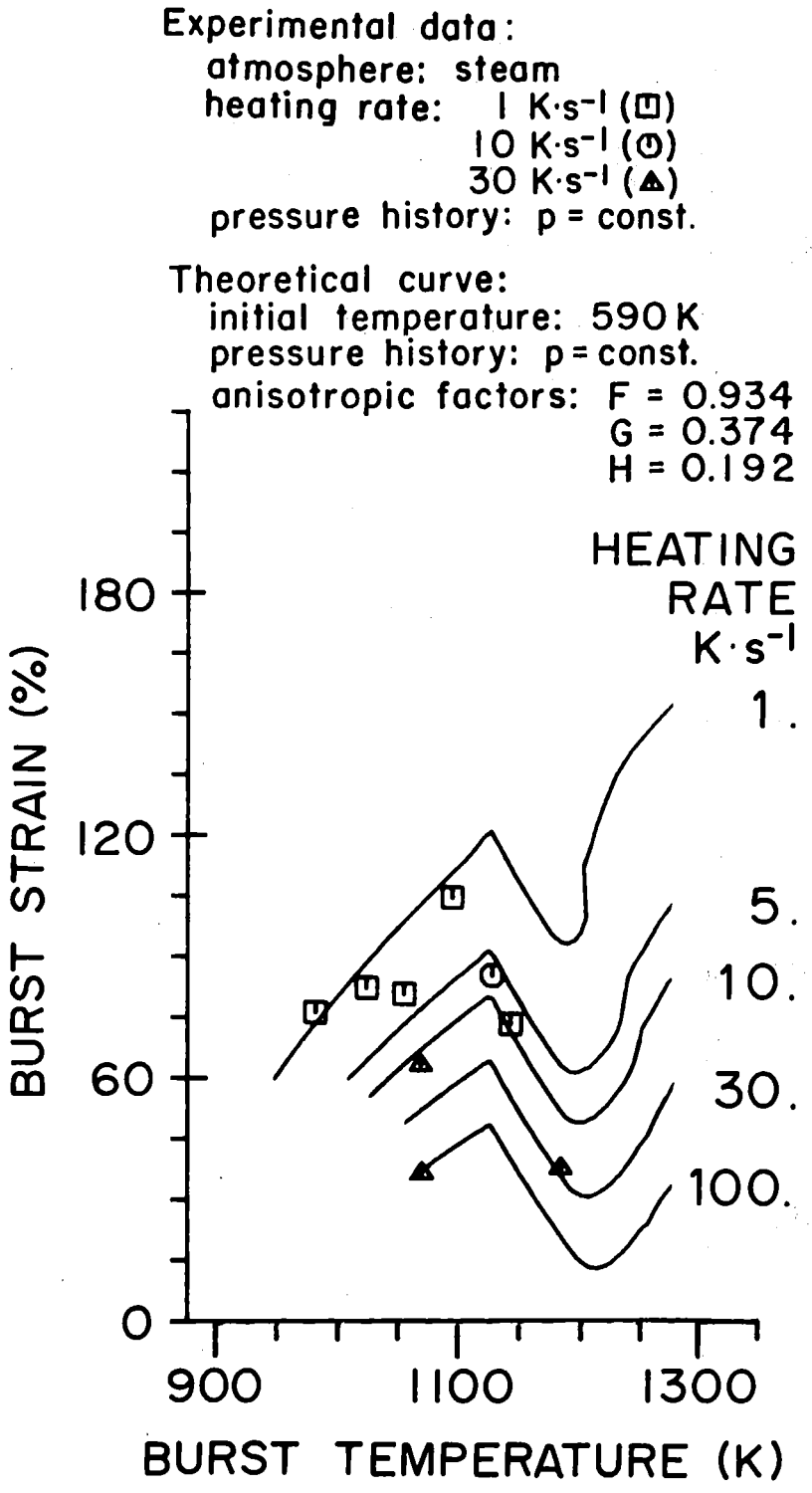

FIGURE 10: Relationship between Burst Strain and Burst Temperature for Various Heating Rates

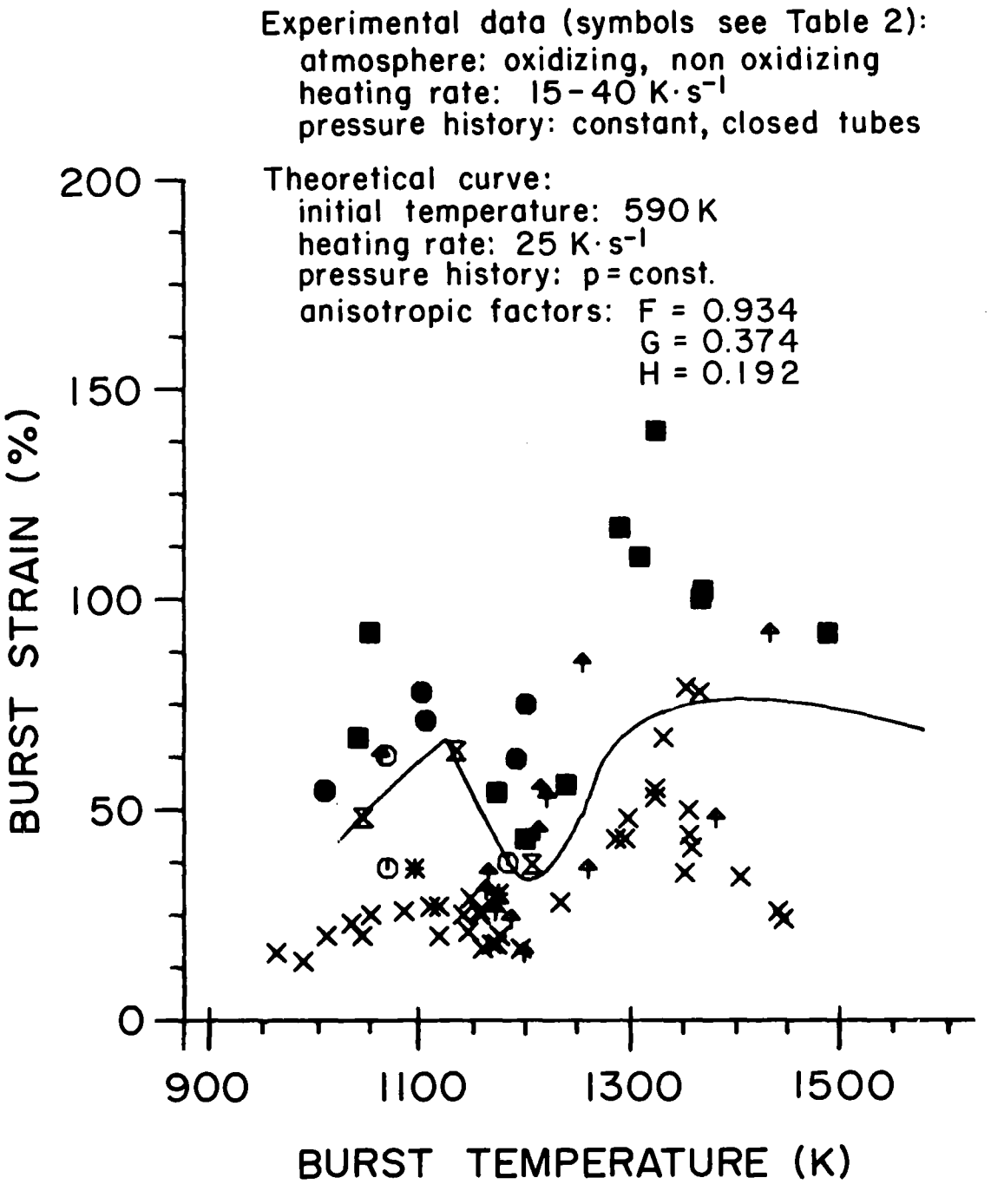

FIGURE 11: Comparison of Experimental Data with Theoretical Curve for Burst Strain versus Burst Temperature.